*Available online at* www.scholarsresearchlibrary.com

**Scholars research library**

**Archives of Applied Science Research, 2011, 3 (5):339-349**
*(http://scholarsresearchlibrary.com/archive.html)*

**ISSN 0975-508X**
**CODEN (USA) AASRC9**

# Structural, Optical and Electrical Properties of Nano-crystalline Hg(SSe) Semiconductor Alloy Thin Films

**V. M. Bhuse**

*Thin Film Research Laboratory, Department of Chemistry, Government Rajaram College, Vidyanagar, Kolhapur, Maharashtra, India.*

---

## ABSTRACT

*The stiochiometric Mercury sulphide selenide alloy, Hg(SSe), have been grown onto glass substrates at 300K for the first time, in the most stable thin film form by employing a chemical bath deposition method. The 'as grown' films were characterized by using XRD, Optical absorption, Electrical measurements and EDAX techniques. The obtained films are dark red in color, stoichiometric, semiconducting and nano-crystalline in a single cubic phase with columnar disk type (spread cabbage) morphology. The cubic Hg(SSe) alloy films were found stable in contrast to cubic HgS. The study of optical property revealed the presence of a single optical band gap at 2.1 eV obeying direct transition law. The dark dc electrical resistivity was found to be of the order of* $10^2$ *ohm cm. The film exhibits n- type of semi-conductivity.*

**Key words**: Semiconductors, Thin films, B: Chemical synthesis, C: Optical properties, D: X Ray diffraction, Scanning electron microscopy.

---

## INTRODUCTION

The mercury chalcogenides, HgX (X= S, Se, Te) and their solid solution are gaining much popularity in the recent years due to their proven use as a host material in optoelectronic applications such as photo conductor, IR detector, emitter, tunable lasers, thermoelectric coolers, electrostatic imaging, photoelectric conversion device and in catalysis [1-8]. The mercury chalcogenides exhibit unusual structural and electrical properties as compared to other members of the group viz. cadmium and zinc chalcogenides [9, 10]. The mercury sulphide (HgS), a technologically important material in quantum electronics [11], exhibit two structural modifications, α HgS (Cinnabar, red, hexagonal structure) and β HgS (Metacinnabar, black, cubic structure). The former is most stable and behaves as a wide band gap semiconductor while, later in bulk form, like mercury selenide (HgSe) and telluride (HgTe) is semimetal due to inverted band structure. The β HgS is metastable and is known to transforms to a stable α HgS even at room temperature [12, 13].

It is well established that the properties of material in thin film form differ significantly from those of bulk [14]. The variations are related to restriction in the three dimensional growth of crystal during thin film formation that usually leads to formation of microcrystalline and nanocrystalline phase having small crystallite size. The ‘smallness’ of crystallite size makes the radial changes in the electronic state of the material affecting the optoelectronic properties of material in profound way, called quantum size effect (QSE). The exact ‘critical size’ after which the quantum size effect can appear is largely determined by the physico-chemical nature of the material and can vary from 0.5 (CuCl) to 46 (PbSe) or more nanometers [15]. The SQE depends upon the radius of exciton (Bohr radius), static permittivity and effective masses of the charge carriers. For mercury chalcogenides, Bohr radius of exciton ($a_B$), static permittivity are all higher while the effective masses are relatively small so that QSE can be seen not only for micro / nanocrystalline thin films but also for larger dimension crystallites [16]. The cubic modification of HgS and HgSe are known to dissolve substitutionally in all the concentrations ranges [17] with the properties varying smoothly between those of the extremes. This compositional variations coupled with quantum confinement effect could give a very large degree of freedom in positioning the optical band gap and other properties as well for broad potential application purpose [18].

In view of this, we planned to deposit Hg(SSe) alloy film using aqueous chemical route and investigate the characteristics like structure, optical and electrical properties. The aqueous chemical route has recently emerged as a cheap, easy and large area accessible technique for growing alloy kind thin films[19,20] and particularly for mercury chalcogenides, due to their large ionicity, the method could give good quality nanocrystals [21].

## MATERIALS AND METHODS

### *2.1 Preparation of anionic precursor solution*

All the solutions were prepared in deionized water using Analytical grade chemicals. A (0.25 M) mixture of Sodiumselenosulphate ($Na_2SeSO_3$) and thiosulphate ($Na_2SSO_3$) was prepared by refluxing 1 g of Sulfur powder, 2.5 g Selenium powder with 8 g anhydrous sodium sulphite in 250 ml distilled water for 9 hours at $90^0$C temperature [17]. The resulting mixture was used as a source of anion ($S^{-2}+Se^{-2}$). It was stored in an air tight container.

### *2.2 Preparation of thin films*

Commercially available Glass slides (size-75*25*2mm), cleaned using chromic acid followed by deionized water were used as substrate to deposit Hg(SSe) thin films. For deposition, 10 ml of (0.25M) mercury nitrate solution, complexed with 25ml of (1M) aqueous ammonia was mixed with 10 ml of anionic precursor solution in a 250 ml capacity beaker at $5^0$C temperature. The final volume of the reaction mixture was made to 180 ml using previously cooled double distilled water. The glass substrates were mounted vertically on specially designed substrate holder (radius- 25 mm) and rotated in solution with a speed of 45±5 rpm. The temperature of the bath was then allowed to increase up to $27^0$C slowly. After about three hours, the slides were removed, washed with deionized water, dried naturally and kept in dark desiccator over $CaCl_2$.

### *2.3 Characterization techniques*

The X-ray pattern of films were recorded on Philips PW-1710 with Cu K$\alpha_1$ line (1.54056Å). The specific resistance was recorded using two probe method in 300-500K temperature range using Zintek-502BC Milliohmmeter. The optical absorption spectra were recorded in wavelength range of 350-950 nm using a Hitachi-330 (Japan) double beam spectrophotometer at room temperature. A Cambridge Stereo Scan (USA) Scanning Electron Microscope (SEM) attached with energy dispersive spectrometer was used to observe surface morphology and for compositional analysis of elements.

## RESULTS AND DISCUSSION

### 3.1. Growth and Physical Properties

The decomposition of a moderately stable mixture of Sodiumselenosulphate and thiosulphate was made possible in aqueous alkaline NaOH medium at pH = 10.4 to give $Hg^{+2}$ and $S^{-2}$, $Se^{-2}$ ions respectively. As the solubility products of HgS and HgSe are low ($K_{sp}$ of HgS = $10^{-47}$ & $K_{sp}$ of HgSe =$10^{-59}$ at $27^0$C) and depend on temperature, control over ion concentrations and hence growth can be achieved by controlling the temperature. At $5^0$C temperature almost all ions are in complexed / bound state, however few of the precursor molecules may dissociate to give few ions. These bare ions get sufficient space and time to combine on substrate (and also in bulk of solution) to produce nuclei (Nucleation). Further, slow increase in temperature facilitates the release of ions from complexed / bound state and diffusion for further growth giving film on substrate and a precipitate in bulk of solution. This process involves formation of film (and precipitate) by building up of ions via the nucleation and growth processes. This ion by ion method helps in maintaining the stoichiometry of mercury chalcogenides in contrast to other high temperature methods.

The mechanism of alloy formation involves the following sequential reactions;

$$Na_2SeSO_3 + 2OH^- \rightarrow Na_2SO_4 + H_2O + Se^{-2} \quad ...(1)$$
$$Na_2SSO_3 + 2OH^- \rightarrow Na_2SO_4 + H_2O + S^{-2} \quad ...(2)$$
$$n\,[Hg(NH_3)_4]^{2+} + {}^{n}/_{2}\, S^{-2} + {}^{n}/_{2}\, Se^{-2} \rightarrow HgS_{0.5}Se_{0.5} + 4n\, NH_3(aq) \quad ...(3)$$

The overall reaction can be written as;

$$n[Hg(NH_3)_4]^{2+} + Na_2SeSO_3 + Na_2SSO_3 + 4OH^- \rightarrow HgS_{0.5}Se_{0.5} + 4n\, NH_3(aq) + 2H_2O \text{ --(4)}$$

The optimized parameters to get good quality films are 0.25 M reactant concentration, pH : 10.4, initial temp.: $5^0$C, Final temperature: $27^0$C, Stirring rate: 45±5 rpm. The color of Hg(SSe) films was found to be dark red.

### 3.2 Structural and Morphological Investigations

Mercury sulphide is an exception among mercury chalcogenides. The cubic structure which is stable for HgSe and HgTe at room temperature is turned out to be unstable for HgS. The hexagonal HgS (i.e. α HgS) is considered as most stable form of HgS, therefore any deposits of cubic HgS (i.e. β HgS) transforms naturally to α HgS [12,13]. This metastable β HgS, however, can forms stable solid solutions with HgSe in cubic structures in whole range of compositions

[17]. The HgS and HgSe can exhibit different structural modifications; therefore, the structural analysis of the as deposited film was performed manually by comparing the obtained XRD peak pattern with those given in JCPDS cards of cubic and hexagonal HgS and HgSe. The XRD pattern of as deposited HgSSe thin film is shown in Fig. 1. The comparison of peaks with those given in JCPDS cards showed a perfect match to cubic form of both HgS and HgSe. The peak positions were found to fall fairly midway to those of cubic HgS (JCPDS card No 06-261) and cubic HgSe (JCPDS card No 08-0469), indicating that Hg(SSe) has been formulated as solid solution. The observed peaks at $2\theta$ of 25.83, 29.93, 42.93, 50.73, 53.35, 62.85, 68.52 degrees therefore can be assigned as the reflections originating from 111, 200, 220, 311, 222, 400 and 331 planes of Hg(SSe) respectively. The XRD pattern showed no peaks corresponding to any hexagonal modification. The XRD pattern of the same alloy film taken after four month showed no sign of post depositional structural transformation confirming the stability of alloy in the cubic phase (XRD not shown). This is in contrast to the bulk behavior where cubic form is considered as unstable [12,13]. The justification of this structural stability stems toward the fact that naturally occurring HgS, if contain transition atoms as impurity (e.g. Iron) or any substitutional selenium ions (in place of S) would exhibit extremely stable cubic modification, called Metacinnabar [13]. This fact provides a new path to grow different solid solutions based on technologically important HgS. The Hg(SSe) pattern showed sharp peaks indicating good crystallinity of the deposit even at room temperature. The high degree crystallinity is attributed to high ionicity of the HgS and HgSe.

A scanning electron microscope of (HgSSe) thin films at X15000 magnification with a scale bar of length 1 μm is shown in Fig.2. The SEM micrograph shows a polycrystalline, uniformly distributed columnar disc like texture (like a spread cabbage). The film is nonporous and compact in appearance. The average crystalline size of a cauliflower, estimated using Cotrells method [22] was found to be 100 nm with disc thickness roughly 60 Å.

The average grain size of Hg(SSe) film can be estimated from the peak width at half maximum of the strongest 111 peak using Scherrer equation;

$$t = 0.9\lambda / B \cos\theta \qquad \ldots(5)$$

Where $\lambda$ is wavelength of x ray used, B is the half angular width in radian at half maximum of peak and $\theta$ is Braggs angle. The calculation yields an average grain size of ~ 60Å. The compositional analysis of film showed Hg: S: Se ratio 1:0.52:0.48 indicating a little deficiency of selenium.

The values of lattice constant (a) corresponding to different planes were obtained by using relation;

$$1/d^2 = (h^2+k^2+l^2)/a^2 \qquad \ldots(6)$$

Where d is the interplanar spacing in angstrom unit, h,k,l are Miller indices.

The accurate lattice constant (a) of Hg(SSe) have been computed from Nelson-Riley plot [4], which is a plot of error function $F(\theta)=\cos^2\theta[1/2 \sin\theta + 1/2\theta]$, ($\theta$ = Braggs diffraction angle) Vs.

lattice constants (obtained from various planes of cubic film using equation 6). The interpolation of line to x axis gave a value of lattice parameter a = 5.949 Å which is more or less free from systematic error (plot not shown). The obtained value is in good agreement with the value of 5.963 Å reported by Voronin et al [23] for $HgS_{0.5}Se_{0.5}$ single crystal. They observed almost linear decrease in the unit cell parameters of the HgSSe system with the increase in selenium content, therefore, assuming that the alloy obeys the Vagard law of composition, we have estimated the stoichiometry of the film using the following equation;

$$a_{(x)} = (x)\, a_{HgSe} + (1-x)\, a_{HgS} \qquad \ldots(7)$$

The value of compositional parameter (x) was calculated to be 0.488 which in good agreement with results of compositional analysis indicating fair stoichiometry of the deposits. The crystallographic parameters of Hg(SSe) thin film, grain size etc are displayed in Table-1.

## 3.3 Optical properties

The absorption spectrum of as deposited Hg(SSe) film recorded at room temperature is shown in Fig. 3. It exhibits the presence of a single absorption edge in the 500-700 nm range. No other absorption except the band edge was observed indicating the absence of any excitonic absorption [16]. The absorption coefficient (α) was found to be of the order of $10^4$ $cm^{-1}$. The data in the vicinity of an absorption edge were analyzed by using the following equations, obeyed at hν > Eg [19] ;

$$\alpha h\nu = A\,(h\nu - Eg)^{r} \qquad \ldots(8)$$

Where, the symbols have their usual meanings. The exponent r depends upon the type of transitions and has values of 1/2 for direct, and 2 for indirect transitions. For valid r, $(\alpha h\nu)^{1/r}$ Vs hν plot shows linear dependence for photon energies greater than band gap (Eg) so that the extrapolation of straight line portions to zero absorption gives energy gaps. Accordingly $(\alpha h\nu)^2$ Vs. hν plot (Fig.4) shows a best fit for r = ½, with a direct gap estimation at 2.1 eV. The band gap measurements for same film after four month do not register any appreciable shift in the values.

The mercury chalcogenides exhibit large ambiguity in their optical properties. The bulk HgSe and β HgS although considered as semimetal (due to their inverted band structure), there are several reports that make these materials semiconductor.. A significant deviation in the values of their optical band gaps have been reported by many authors [2-4,7,12,14,16,24-31]. A strong blue shifting in band gap of mercury chalcogenides (by several electron volts) due to their larger Bohrs radius of excitons have been reported by Nedeljkovic [24]. As high as 3.15 eV have been reported for HgSe colloidal particles of average size of 3 nm. Thin films of chalcogenides deposited at low temperature mostly exhibit nanocrystalline size due to strong size quantization [15-16,18]. For HgSe thin film of ~8 nm crystallite size grown by using chemical bath method, a value of 2.5 eV have been reported by Pejova et al [25]. The crystallite size in the above case was calculated on the basis of FWHM of XRD peaks using Debye-Scherrer equation. For amorphous HgSe film, Pramanik et al [26] reported the band gap at 1.42 eV. The polycrystalline HgSe thin films obtained using reactive solution grown techniques [2,4] were reported to have a band gaps of magnitude ~0.8 eV for crystallites of ~30 nm size, while HgSe thin film with ~42 nm crystallites size obtained from electrochemical atomic layer epitaxy method have exhibited a gap of 0.88 eV [27]. Whether β HgS is a semimetal has been the subject of controversy till date as both positive and negative band gaps are reported in the literature. The calculations based on the density functional theory within the local density approximation (LDA) suggested that cubic HgS phase is actually a semiconductor, and not a semimetal [9, 21]. A strong shifting of absorption edge from NIR to UV-VIS region have been observed by Wang and Zhu [7] for β HgS of an average size 13 nm, prepared using sonochemical method. The nano-particles of β HgS with an average size ~ 15 nm prepared via wet chemical method has shown the band gap tuning in visible region with the measured gap at ~1.38 eV [16]. Similar blue shifting to 2.6 eV has been reported by Ding et al [31] for 10 nm particles size. In general, for HgSe, HgS and Hg(SSe) materials, either in the form of thin films or nanoparticles, the reported values are all higher and nonzero indicating a strong blue shifting of band gaps. The observed large deviations in each case can be attributed to varying degrees of quantum size effects. Besides the strong SQE, the influence of other factors such as spin orbit coupling, large density of dislocations, local inhomogeneity, changes in the nature of the conduction band in thin film form, presence of neutral/ionized impurities (V defect) cannot be denied.

### 3.4 Electrical and Thermo-electrical Properties

The electrical resistance of Hg(SSe) thin films of 0.71 μm thickness was measured between two silver pasted electrodes, 1 cm in length and 1 cm apart. The specific conductance was found to be $1.96 \times 10^{-3}$ $Ohm^{-1}$ $cm^{-1}$ at room temperature. The temperature dependence of dark conductivity, σ, is represented in Fig. 5. It can be seen that the dark conductivity increases with increase in temperature. The increase in conductivity exhibit two different lines in log σ against 1000/T plot corresponding to two kinds of variations, a trend as such is commonly seen in many semiconductor thin films. The low temperature variation region is called extrinsic (impurity) conduction region where a variable range hopping conduction due to ionized impurities dominates while, a high temperature variation region, a characteristic of an intrinsic conduction, is due to grain boundary scattering limited conduction mechanism. The conduction activation energy was calculated using the following relation;

$$\sigma = \sigma_0 \exp(-Ea/kT) \qquad \ldots(9)$$

Where, the symbols have their usual meanings. The activation energy obtained from the linear portion of the graphs was found to be 0.374 eV and 0.114 eV for Hg(SSe) at high temperature and low temperatures respectively. In thermoelectric power measurements, the open circuit thermo voltage generated due to temperature gradient across a length of sample was found to have negative terminal connected at the cold end, corresponding to presence of majority negative charge carriers indicating n type nature of the alloy.

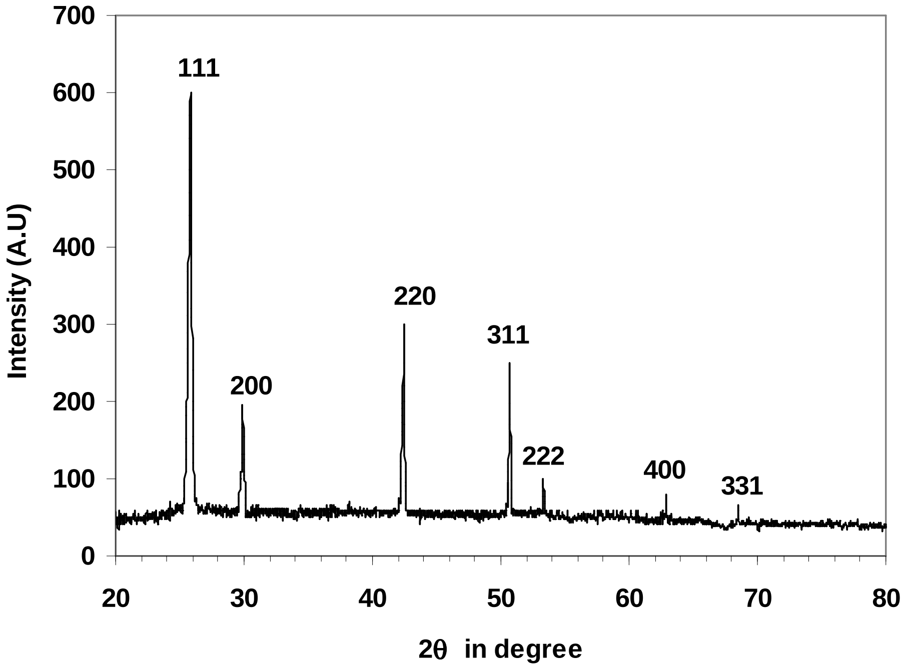

**Fig.1:** XRD Pattern of as deposited Hg(SSe) films.

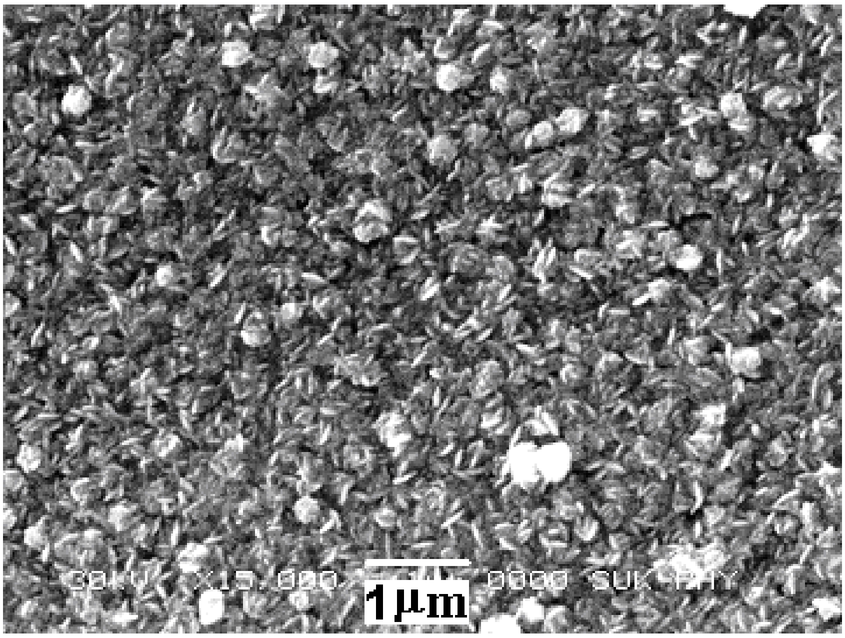

**Fig.2:** Scanning Electron Micrographs of as deposited Hg(SSe) film at X15000 magnification.

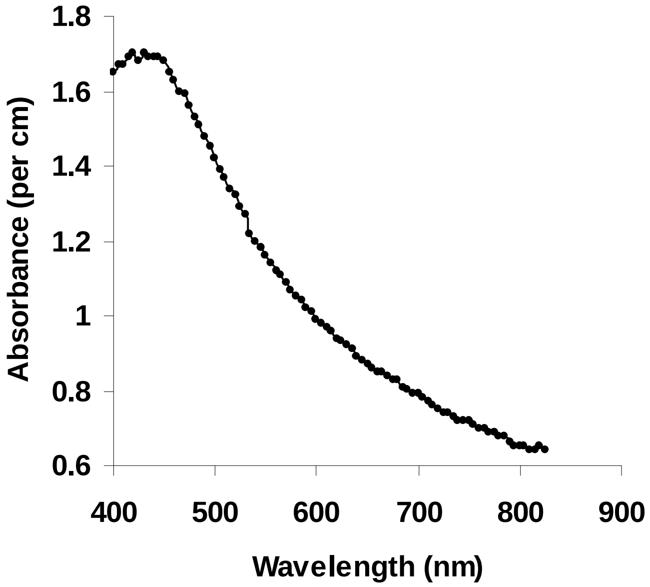

**Fig.3:** **Absorption spectra of Hg(SSe)**

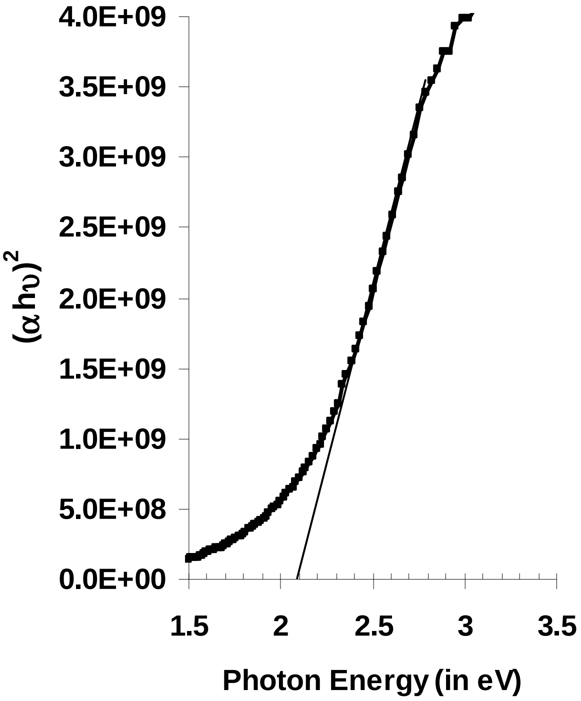

**Fig.4:** **A plot of $(\alpha h\nu)^2$ Vs hν for Hg(SSe)**

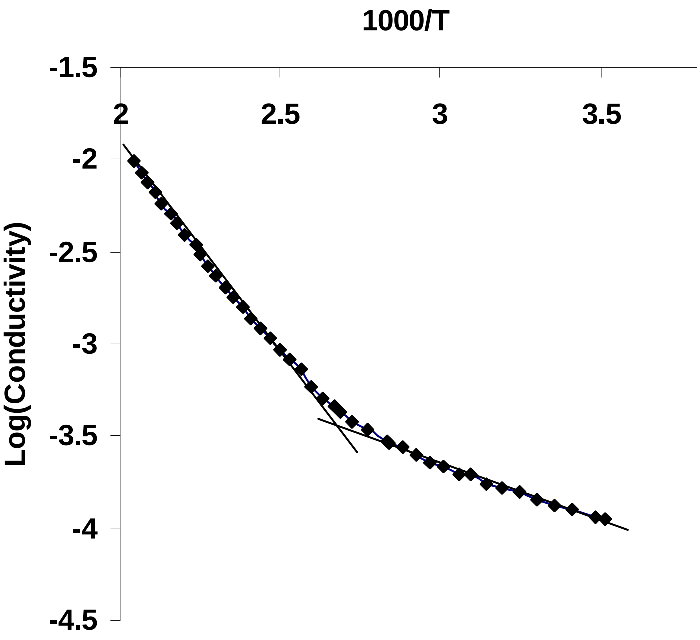

**Fig.5:** The variation of log (conductivity) with inverse of absolute temperature for Hg(SSe)

**Table-1:** Various Parameters of Hg(SSe) thin films

| Observed d values | hkl plane assigned | Cell Size in $A^0$ (From N-R plot) | Grain Size in $A^0$ | Band gap (in eV) | Film Thickness in μm | Activation Energy LT &HT |
|---|---|---|---|---|---|---|
| 3.4462 | 111 | | | | | |
| 2.9828 | 200 | | | | | |
| 2.1285 | 220 | | | | | |
| 1.7981 | 311 | 5.949 | 60 | 2.1 | 0.71 | 0.114(L.T) |
| 1.7158 | 222 | | | | | 0.374(H.T) |
| 1.4773 | 400 | | | | | |
| 1.3682 | 331 | | | | | |

## CONCLUSION

A ternary Hg(SSe) alloy system can be deposited in a stable cubic modification at low temperatures by a chemical deposition technique easily. The films are stoichiometric nanocrystalline with cabbage type morphology. The optical studies revealed the presence of band gap at 2.1 eV exhibiting strong quantum size effect.

The films are n type semiconductors at room temperature with resistivity of the order of $5.3 \times 10^2$ Ω cm. The compositional variation coupled with strong size quantization in mercury chalcogenides is a promising material for broad radiation detection application purpose.

---

**Acknowledgement**

The author V.M. Bhuse thankfully acknowledges Hon. Director, Department of Higher Education, Pune, Maharashtra (India) for his constant support in research activity.

## REFERENCES

[1] K.A. Higginson, M. Kuno, J. Bonevich, S.B. Qadri, M. Yousuf, H. Mattoussi, *J. Phys. Chem.* **2002**, B 106(39), 9982.
[2] S.Y. Girgis, A.M. Salem, M.S. Selim, *J. Phys: Condens. Matter*, **2007,** 19, 116213.
[3] V. Vankatasamy, N. Jayaraju, S.M. Cox, C. Thambidurai, M. Mathe and J.L. Stickney, *J. Electroanal. Chem*, **2006**, 589, 195.
[4] P.P. Hankare, V.M. Bhuse, K.M. Garadkar, A.D. Jadhav, *Mater. Chem. Phys*, **2001**, 71, 53.
[5] C.R. Whisett, J.G. Broerman, C.J. Summers, in: R.K. Willardson, A. C. Beer (Eds.), Semiconductors and Semimetals, Vol.16, Academic Press, New York, **1981**, Ch-4.
[6] N. Tokyo, *J. Appl. Phys*, **1975**, 46, 4857.
[7] H. Wang, J.J. Zhu, *Ultrason. Sonochem*, **2004**, 11, 293.
[8] Y. T. Park, S. G. Lee, Y.U. Kim, *Int. J. Hydrogen Energy,* **1995**, 20, 711.
[9] A. Delin, A. Salam, *Phy. Rev. B*, **2002,** 65, 153205.
[10] G. G. Roberts, R. Zallen, *J. Phys. C: Solid State Phys*, **1971**, 4, 1890.
[11] M. Shao, L. Kong, Q. Li, W. Yu, Y. Qian, *Inorg. Chem. Commun*, **2003,** 6, 737.
[12] S.B. Qadri, M. Kuno, C.R. Feng and B.B. Rath, *Appl. Phy. Lett.* **2003**, 83(19), 4011.
[13] B.J Kowalski, W. Szuszkiewicz, B.A. Orlowski, Z.Q. He, L. Ilver, J. Kanski, P.O. Nilsson, *J. Electron spectrosc. Relat. Phenom,* **1997**, 85, 17.
[14] M.M. El-Nahass, F. Abd El-Salam, M.A.M. Seyam, J. Mater. Sci, **2006,** 41, 3573.
[15] A.L. Stroyuk, A.I. Kryukov, S.Y. Kuchmii, V.D. *Pokhodenko, Theor. Exp. Chem*, **2005**, 41(2), 67-91.
[16] B.K. Patel, S. Rath, S.N. Sarangi, S.N. Sahu, Appl. Phys, **2007**, A 86, 447.
[17] C. Zylberajch, A. Ruaudelteixier, A. Barraud, *Thin Solid Films*, **1989**, 179, 9.
[18] S.V. Kershaw, M. Harrison, A.L. Rogach, A. Kornowski, *IEEE J. Sel.Top. Quantum Electron,* **2000,** 6(3), 534.
[19] B.R. Arbad, S.G. Chonde, P.P. Hankare, V.M. Bhuse, *Archives of Applied Science Research*, , **2011,** 3(2), 422.
[20] A.S. Rajbhoj , J.T. Deshmukh, S.T Gaikwad, P.P. Hankare, V.M. Bhuse, *Archives of Applied Science Research*, , **2011,** 3(4), 440.
[21] A. Hao, C. Gao, M. Li, C. He, X. Huang, D. Zhang, C. Yu, H. Liu, Y. Ma, Y. Tian, G. Zou, *J. Phys.:Condens. Matter*, **2007**, 19, 425222.
[22] A. Cottrell, *Introduction to Metallurgy , Arnold, Londan*, **1975,** P.173
[23] V.I. Voronin, V.V. Shchennikov, I.F. Berger, V.P. Glazkov, D.P. Kozlenko, B.N. Savenko, S.V. Tikhomirs, *Phy. Solid State*, **2001**, 43(11), 2165.
[24] J.M. Nedeljkovic, M.T. Nenadovic, O. I. Micic, A.J. Nozik, *J. Phys. Chem,* **1986,** 90(1), 12-13.
[25] B. B. Pejova, M.Z. Najdoski, I. S. Grozdanov, S. K. Dey, *J. Mater. Chem*, **1999**, 9, 2889.
[26] P. Pramanik, S. Bhattcharya, *Mater. Res. Bull,* **1989**, 24, 945.
[27] M.K. Mathe, S. M. Cox, V. Venketasamy, U. Happek, J.L. Stickney, *J. Electrochem. Soc,* **2005**, 152(11),751.
[28] S. Rath, S.N. Sahu, *Eur. Phys. Lett*, **2004,** 67, 294.

[29] A. L. Rogach, A. Kornowski, S. V Kershaw, M. G. Burt, M. T. Harrison, A. Eychmuller, H. Weller, *Adv. Mater*, **1999,** 11, 552.
[30] S. Rath and S.N. Sahu, *Journal Metastable and Nanocrystalline Materials*, **2005**, 23,125.
[31] T.Ding, Jun-Jie Zhu, *Mat. Sci & Engg*, **2003,** B100, 307.